ADVANCES IN ATMOSPHERIC SCIENCES, VOL. 30, NO. 3, 2013, 779–789

A New Weighting Function for Estimating Microwave Sounding Unit Channel 4 Temperature Trends Simulated by CMIP5 Climate Models

ZHANG Xuanze[1,2] (张选泽), ZHENG Xiaogu*[1] (郑小谷), YANG Chi[1] (杨 赤), and LUO San[1] (骆 三)

[1] *College of Global Change and Earth System Science, Beijing Normal University, Beijing* 100875

[2] *College of Atmospheric Sciences, Lanzhou University, Lanzhou* 730000

(Received 13 July 2012; revised 28 November 2012)

ABSTRACT

A new static microwave sounding unit (MSU) channel 4 weighting function is obtained from using Coupled Model Inter-comparison Project, Phase 5 (CMIP5) historical multimodel simulations as inputs into the fast Radiative Transfer Model for TOVS (RTTOV v10). For the same CMIP5 model simulations, it is demonstrated that the computed MSU channel 4 brightness temperature (T4) trends in the lower stratosphere over both the globe and the tropics using the proposed weighting function are equivalent to those calculated by RTTOV, but show more cooling than those computed using the traditional UAH (University of Alabama at Huntsville) or RSS (Remote Sensing Systems in Santa Rosa, California) static weighting functions. The new static weighting function not only reduces the computational cost, but also reveals reasons why trends using a radiative transfer model are different from those using a traditional static weighting function. This study also shows that CMIP5 model simulated T4 trends using the traditional UAH or RSS static weighting functions show less cooling than satellite observations over the globe and the tropics. Although not completely removed, this difference can be reduced using the proposed weighting function to some extent, especially over the tropics. This work aims to explore the reasons for the trend differences and to see to what extent they are related to the inaccurate weighting functions. This would also help distinguish other sources for trend errors and thus better understand the climate change in the lower stratosphere.

Key words: CMIP5, RTTOV, MSU weighting function, lower stratospheric temperature variability

Citation: Zhang, X. Z., X. G. Zheng, C. Yang, and S. Luo, 2013: A new weighting function for estimating microwave sounding unit channel 4 temperature trends simulated by CMIP5 climate models. *Adv. Atmos. Sci.*, **30**(3), 779–789, doi: 10.1007/s00376-013-2152-x.

1. Introduction

There is a large amount of compelling scientific evidence showing that human activities have influenced global climate variability over the past 150 years (Santer et al., 2005; Wigley et al., 2006; IPCC, 2007). However, large uncertainties relating to temperature variability in the upper atmosphere, caused by the complex procedure of adjusting raw measurements for inhomogeneities, still remain (Thorne et al., 2005a). Studies of air temperature variability help us to better understand the anthropogenic influence on climate change (Santer, 1996).

Satellite-based microwave sounding unit (MSU) and advanced microwave sounding unit (AMSU) sensors have provided about 30 years of records on atmospheric layer temperature since November 1978, when the Next-generation Television and Infrared Operational Satellite (TIROS-N) carrying the first MSU was launched. These records have been further adjusted to provide continuous and stable data which may be suitable for monitoring changes in climate atmospheric temperature (Spencer and Christy, 1992a, 1992b; Mears and Wentz, 2005; Zou et al., 2006). Meanwhile, the Coupled Model Inter-comparison Project, now in its fifth phase (CMIP5), performs extensive simula-

*Corresponding author: ZHENG Xiaogu, x.zheng@bnu.edu.cn

tions of historical climate, including temperature variability in the lower stratosphere.

Although almost all satellite observations and historical simulations of coupled climate models (Douglass et al., 2004; Wigley et al., 2006; Douglass et al., 2007; Santer et al., 2008) have captured the cooling trend in the stratosphere, the estimated trend magnitudes differ significantly (Seidel et al., 2004; Thorne et al., 2005b). By analyzing the difference between satellite observations and model simulations of stratospheric temperature, not only can we test the current theory about anthropogenic influence on climate change, but we can also evaluate the reliability of those observations.

This study focuses on a comparison of historical simulations by CMIP5 GCMs and satellite-based MSU brightness temperature series in the lower stratosphere (i.e. T4). To facilitate comparisons with the actual MSU deep-layer temperature T4, two approaches are used to generate MSU-equivalent temperature from multimodel simulations. One approach is to use a static weighting function (Spencer and Christy, 1992a, 1992b; Santer et al., 1999, 2000, 2005; Steiner et al., 2007), and the other is to simulate MSU T4 with a fast radiative transfer code (Saunders et al., 1999). Santer et al. (1999) concluded that for temperature changes averaged over large areas, MSU-equivalent temperatures calculated using static global weighting functions gave a similar result as those using a radiative transfer code. Differences between the linear trends of MSU-equivalent temperature generated by the two approaches were found to be less than 0.02 K $(10\ \mathrm{yr})^{-1}$ on global scales. However, the radiative transfer code used by Santer et al. (1999) is an old version [based on Grody (1983)] with low vertical resolution and lacking enough accuracy in terms of transmittance to the top of pressure in the stratosphere. Steiner et al. (2007) tested the validity of generating MSU-equivalent T4 temperature from CHAMP RO (Global Navigation Satellite System radio occultation (RO) observations of the CHAllenging Minisatellite Payload for geoscientific research (CHAMP) satellite) profile data by using the fast Radiative Transfer Model for TOVS (RTTOV) v8.5 and a static weighting function, and concluded that the difference between the brightness temperatures T4 using the two methods was less than 0.2 K on global scales. However, the difference between temperature trends was not discussed.

In this paper, CMIP5 simulated monthly MSU-equivalent brightness temperature T4 is calculated using the latest fast radiative transfer model RTTOV v10 for further improving simulation. Weighting functions provided by the University of Alabama at Huntsville (UAH) (Spencer and Christy, 1992a) and Remote Sensing Systems in Santa Rosa, California (RSS) are also applied to the CMIP simulated atmospheric temperature for obtaining monthly multimodel MSU temperature. It is found that the T4 trends of multimodel simulations computed using the RSS (or UAH) weighting function are about -0.04 K $(10\ \mathrm{yr})^{-1}$ [or -0.03 K $(10\ \mathrm{yr})^{-1}$] less than those calculated by RTTOV v10.

Intuitively, RTTOV should give more physically-based and accurate T4 simulations, while the weighting function approach is computationally cheaper and easier to apply. Therefore in this study, a new weighting function, converted from multimodel transmittance estimated by RTTOV for MSU T4, is proposed. The new weighting functions are then applied to compute MSU T4 trends simulated by CMIP5 models on global scales. It is found that these simulated trends are consistent with those calculated by RTTOV directly.

The paper proceeds as follows. Section 2 briefly introduces the 11 CMIP5 models for the historical experiment, three groups of MSU observations [UAH v5.4, RSS v3.3 and the version 2.0 of the National Oceanic and Atmospheric Administration (NOAA) National Environmental Satellite, Data and Information Service (NESDIS) Center for Satellite Applications and Research (STAR) (Zou et al., 2006, 2009)] and RTTOV v10. Section 3 describes the two methods for the computation of MSU-equivalent T4 and an autoregressive model of order one (AR-1) for the linear trend estimation for T4 anomaly series. Section 4 presents the results of the weighting functions and multimodel simulated trends using those weighting functions and RTTOV v10. In section 5, we discuss the consistency of trends estimated using satellite observations and CMIP5 multimodel historical simulations, and compare the differences among simulated trends using the UAH weighting function, RSS weighting function, the proposed weighing function, and those calculated by RTTOV.

2. Data and model

2.1 *MSU/AMSU brightness temperature*

The TIROS-N series satellites carrying the MSU/AMSU instrument have provided about 30 years of atmospheric layer temperature records since late 1978. The MSU has four oxygen absorption band channels with center frequencies at 50.30, 53.74, 54.96, and 57.95 GHz, respectively. Channels 2, 3 and 4 correspond to the temperature in the middle troposphere, the troposphere/stratosphere, and the lower stratosphere, respectively. Beginning in 1998, the MSU has been replaced by the AMSU (the NOAA K, L, M, N series and MetOp-A). The AMSU contains more chan-

nels than the MSU, and the AMSU channels (channels 5, 7 and 9) have similar frequencies to those (channels 2, 3 and 4) of the MSU sensor (Christy et al., 2003). In this paper, the lower stratospheric brightness temperature constructed using MSU channel 4 and AMSU channel 9 are denoted by T4.

However, owing to calibration error, orbital decay, inaccurate local equator crossing time, warm target, the stratospheric cooling contributions, bias in different satellite measurement systems, channel changes in the MSU and AMSU etc., the original T4 needs to be extensively reprocessed (Mears et al., 2003; Zou et al., 2006). There are four groups involved in such calibration research: groups at the UAH (Spencer and Christy, 1990, 1993; Christy et al., 2007), at the RSS (Mears et al., 2003; Mears and Wentz, 2005, 2009), at the NOAA/NESDIS (Zou et al., 2006, 2009), and at the University of Maryland (UMd) (Vinnikov and Grody, 2003; Grody et al., 2004; Vinnikov et al., 2006). The T4 time series produced by the first three groups are shown in Fig. 1.

Figure 1 shows that the agreement among the three groups' results is reasonable, and that they all pick up the two warming-up peaks in the T4 time series as the responses to two volcanic eruptions (i.e. El Chichon in 1983 and Mount Pinatubo in 1991). Because the latter eruption was strong, the maximum warming peak in T4 near 1992 was about 1.5 K on the global scale.

2.2 *CMIP5 simulations*

CMIP5 aims to produce a freely available state-of-the-art multimodel dataset designed to advance the knowledge of climate studies. More than 20 modeling groups are performing CMIP5 simulations using about 50 models (Taylor et al., 2012). CMIP5's forcings for historical (1850 to at least 2005) simulations may include: atmospheric composition (including CO_2) due to both anthropogenic and volcanic influences; solar forcing; land use; emissions or concentrations of short-lived species and natural and anthropogenic aerosols (Taylor et al., 2009).

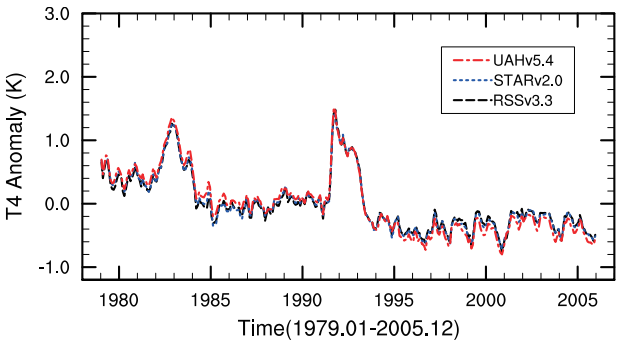

Fig. 1. Time series of global MSU/AMSU T4 anomalies for UAHv5.4 (red), STAR v2.0 (blue), and RSS v3.3 (black), shown for the lower stratosphere temperature. The analysis period is January 1979 to December 2005, the period of maximum overlap between the observations and CMIP5 model historical simulations.

In this study, a set of 33 historical realizations simulated with 11 CMIP5 climate models is used for the comparison study with the satellite-observed T4. Some more detailed information about the CMIP5 models and forcings used in this study is shown in Table 1.

2.3 *RTTOV v10*

RTTOV v10 is the latest development of the fast radiative transfer model for the TIROS Operational Vertical Sounder, as a project of the European Organization for the Exploitation of Meteorological Satellites Numerical Weather Prediction Satellite Application Facility (Saunders et al., 1999; Matricardi et al., 2001; Matricardi, 2005, 2008). Given profiles of atmospheric variables such as pressure, temperature, water vapor, variable gas concentrations, cloud and surface properties (referred to as the model states), the model allows rapid simulations of radiances for satellite infrared or microwave nadir scanning radiometers. The primary role of RTTOV v10 is as an observational operator to connect the model states with brightness temperature observed by the satellite sensoring system. Detailed information about RTTOV v10 can be found at http://research.Metoffice.gov.uk/research/interproj/nwpsaf/rtm/.

RTTOV v10 was originally designed to transfer instantaneous atmospheric state variables into instantaneous brightness temperature. However, in general the outputs of the CMIP5 climate models are monthly. Monthly state variables have to be used as the inputs to RTTOV. Therefore, one needs to know whether the brightness temperature simulated in this way is equivalent to the monthly mean brightness temperature simulated by RTTOV using the instantaneous state variable as the input.

To investigate this problem, we compare the monthly mean of AMSU-A channel 9 brightness temperature simulated by RTTOV using the European Centre for Medium-Range Weather Forecasts (ECMWF) global atmospheric reanalysis (ERA) Interim Reanalysis 6-hour global data as the input, with the brightness temperature simulated by RTTOV using the ERA Interim Reanalysis monthly averaged data as the input, for July 2003 and July 2006 respectively. It turns out that the difference between the former and the latter is less than 0.05 K, and there is no systematic difference. Considering that the instrumental error is 0.3 K, 0.05 K is negligible. The

Table 1. 11 CMIP5 climate model historical (1850–2005) experiments. Detailed information for the abbreviated forcings can be found in Appendix 1.2 at http://cmip-pcmdi.llnl.gov/cmip5/docs/cmip5_data_reference_syntax.pdf.

CMIP5 ID	Institute/Country	Forcings	Resolution (lat × lon × l_p)	Realizations
BCC-CSM1.1	BCC/China	Nat, Ant, GHG, SD, Oz, Sl, Vl, SS, Ds, BC, OC	64×128×17	3
BNU-ESM	GCESS-BNU/China	Nat, Ant	64×128×17	1
CanESM2	CCCma/Canada	GHG, Oz, SA, BC, OC, LU, Sl, Vl (GHG includes CO_2, CH_4, N_2O, CFC11, effective CFC12)	64×128×22	4
CNRM-CM5	CNRM-CERFACS/ France	GHG, SA, Sl, Vl, BC, OC	128×256×17	1
FGOALS-s2	LASG-IAP/China	GHG, SD, Oz, Sl, Vl, SS, Ds, BC, OC	108×128×17	3
GISS-E2-H	NASA-GISS/USA	GHG, LU, Sl, Vl, BC, OC, SA, Oz (also includes orbital change, BC on snow, nitrate aerosols)	90×144×17	5
GISS-E2-R	NASA-GISS/USA	GHG, LU, Sl, Vl, BC, OC, SA, Oz (also includes orbital change, BC on snow, nitrate aerosols)	90×144×17	5
INM-CM4	INM/Russia	N/A	120×180×17	1
MIROC-ESM	JAMSTEC et al./ Japan	GHG, SA, Oz, LU, Sl, Vl, MD, BC, OC	64×128×35	3
MRI-CGCM3	MRI/Japan	GHG, SA, Oz, LU, Sl, Vl, BC, OC (GHG includes CO_2, CH_4, N_2O, CFC-11, CFC-12, and HCFC-22)	160×320×23	4
NorESM1-M	NCC/Norway	GHG, SA, Oz, Sl, Vl, BC, OC	96×144×17	3

AMSU channel 9 (or MSU channel 4) is mainly sensitive to the stratosphere, so water vapour and clouds in the troposphere, which have high temporal variation, have few effects. Therefore in this study, we use the models' monthly outputs as the input to RTTOV v10 for calculating the model simulated monthly mean T4.

Figure 2 shows the T4 time series simulated by the 11 CMIP5 models over 1979–2005. It seems that different models have different responses to various radiative forcing in the stratosphere. For instance, because of the lack of volcanic aerosol forcing in the model INM-CM4 (Institute of Numerical Mathematics Climate Model version 4) (see Table 1), the warming impact did not show up in the years of the two volcano eruptions (blue line in Fig. 2); whereas, some models, e.g. BNU-ESM (Beijing Normal University Earth System Model), BCC-CSM1.1 (Beijing Climate Center Climate System Model version 1.1) and MRI-CGCM3 (Meteorological Research Institute Coupled atmosphere-ocean General Circulation Model version 3) overreacted to the occurrence of the two eruptions, by warming up more than 2 K (see Fig. 1).

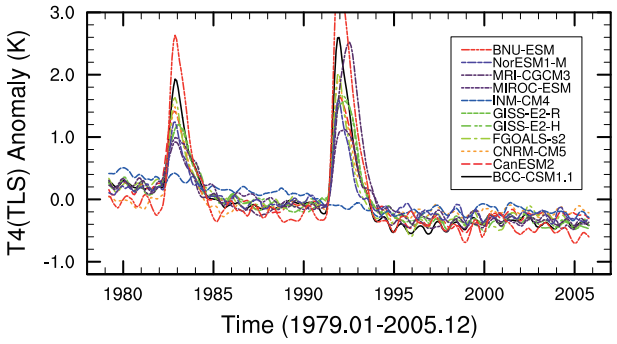

Fig. 2. Time series of T4 monthly anomalies (smoothed by 5-month running mean) for multimodel first realization over 1979–2005. All the models' T4s are calculated by RTTOV v10 directly.

3. Methods

To facilitate comparisons with the actual MSU deep-layer temperature T4, two methods are used to generate equivalent MSU temperature from multimodel simulations. One method is to simulate MSU T4 by a fast radiative transfer code, as mentioned in section 2 (Spencer and Christy, 1992a, 1992b). The other method is to apply a static weighting function to simulated temperature at all model pressure levels (Santer et al., 1999), which is discussed in this section.

3.1 *Weighting function method*

In this paper, two static weighting functions (supplied by RSS and UAH) are used for the MSU T4 estimation. The RSS weighting function was derived using the U.S. standard atmospheric profiles (Mears and Wentz, 2009), and the UAH weighting functions were static mean weighting functions, which is a sim-

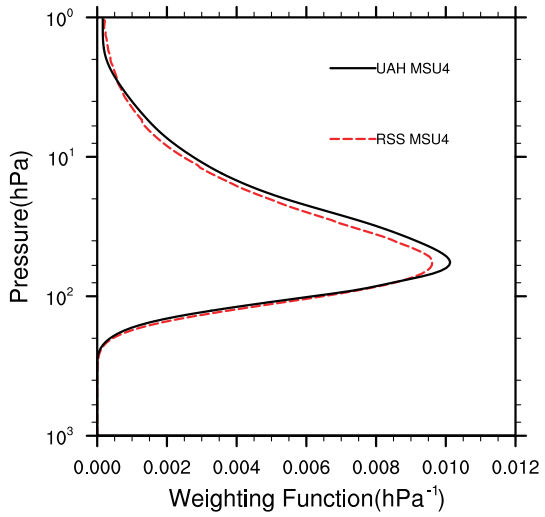

Fig. 3. MSU channel 4 instantaneous weighting functions at nadir. The UAH T4 weighting function was generated from mean static weighting functions for 5 hPa layers provided by J. Christy (Spencer and Christy, 1992a), UAH (black line), and the RSS T4 weighting function was calculated from instantaneous weighting functions of height provided by RSS (red dashed line). The U.S. standard atmosphere, a surface relative humidity of 70%, and a PV scale height of 1500 m, were used.

ple set of geographically and seasonally invariant weights (Spencer and Christy, 1992a). Their vertical distributions at nadir (at about 300 levels) are shown in Fig. 3. The peaks of the two weighting functions are located between 70 hPa and 80 hPa. Since the peak value of the UAH weighting function is larger than that of RSS, the estimated T4 trends could be different if these weighting functions are applied.

Since the vertical levels of models and the levels of weighting functions are different, the weighting functions have to be assigned at the vertical levels of the models. Assuming that model-simulated air temperature T can be represented by a four-dimensional array (x, y, l_p, t), where, the variables x and y (x=1, n_x, y=1, n_y) run over longitude and latitude grid points, l_p index (l_p=1, nl_p) runs over the number of pressure levels of the model, and t is an index over months (1979–2005). From up to the bottom of the model atmosphere, the weight for the l_pth model level is given by

$$W(l_p) = \frac{1}{N(l_p) - M(l_p) + 1} \sum_{i=M(l_p)}^{N(l_p)} w_i(p_{i+1} - p_i) \,, \tag{1}$$

where w_i is the value of a weighting function (Fig. 3) at the ith pressure level, p_i is the responding pressure at the ith pressure level, and $N(l_p)$ ($M(l_p)$) is the pressure level of the weighting function which is most close to the (l_p+1)th ((l_p-1)th) pressure level of the model. Thus, the MSU-equivalent brightness temperature T4 of a model can be simulated as

$$T_{\mathrm{MSU4}}(x, y, t) = \frac{\sum_{l_p=1}^{nl_p} T(x, y, l_p, t) W(l_p)}{\sum_{l_p=1}^{nl_p} W(l_p)} \,, \tag{2}$$

where $T(x, y, l_p, t)$ is the monthly mean temperature simulated using a CMIP5 model.

3.2 *Weighting function derived using RTTOV*

Since the above weighting functions were derived from standard atmosphere and the peak values are quite different, they may not be well representative of the CMIP5 atmospheres. For this reason a new weighting function is derived using the CMIP5 atmospheric profiles, which may be more realistic for the evaluation purpose in this study. From the top to bottom of the atmosphere, the weight of the model for the *plev*th level for a location and a month is calculated by

$$W(l_p) = \frac{1}{2}[\tau(l_p + 1) - \tau(l_p - 1)] \,, \tag{3}$$

where $\tau(l_p)$ represents the transmittance from the specific pressure level to the top of atmosphere (TOA), and is calculated using the RTTOV with the inputs from the CMIP5 model simulations (see Appendix for a more detailed proof). The weighting functions on the global scale for the climate models are defined as spatial and temporal averages of the weights determined using Eq. (3). The MSU-equivalent brightness temperature T4 of a model is derived by substituting W in Eq. (3) for W in Eq. (2).

3.3 *Computation of the linear trend*

The global-mean T4 anomalies from observations (RSS v3.3, STAR v2.0, UAH v5.4) and those calculated using static weighting functions (RSS, UAH, and models) and RTTOV v10 are used to obtain the linear trends over the 27-yr period 1979–2005, inclusive. Since the annual T4 series has temporal correlation, we consider the residual of the T4 series as the red noise series. The red noise assumption may not change the scale of the estimated trend much, but will change the significance of the estimated trend (Jones, 1989; Zheng and Basher, 1999). The trend and its significance can be estimated using the function "arima" in the statistics software *R* (Becker et al., 1988).

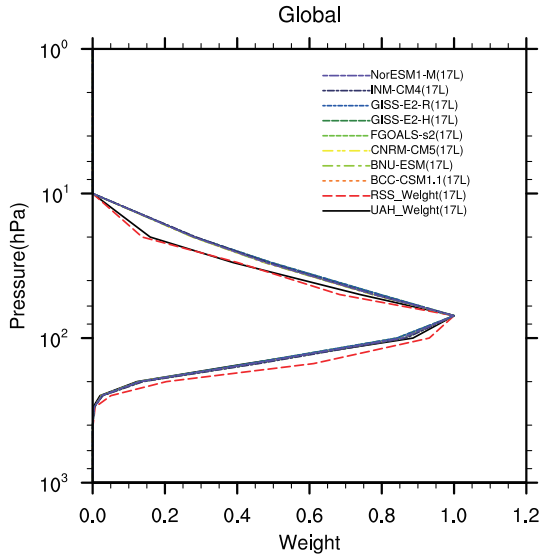

Fig. 4. Normalized weighting functions for UAH (black solid), RSS (red dashed), and climate models (colored dashed) at 17 discrete pressure levels on global scales.

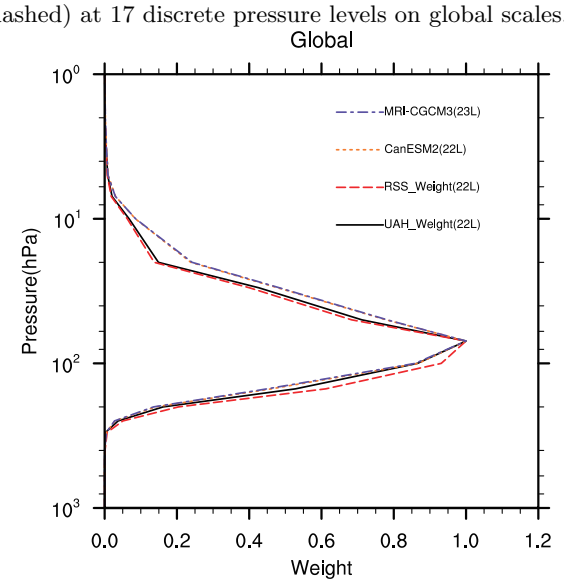

Fig. 5. The same as Fig. 4, but the vertical resolution of the models is 22 pressure levels.

4. Results

4.1 *Weighting functions*

For most of the CMIP5 models used in this study, the top of the model atmosphere is at 10 hPa, and the model has 17 discrete pressure levels. For calculating their weighting functions, each model output is used as the input for RTTOV v10 to estimate the transmittance from each model pressure level to the TOA. For each model, the weighting function for each month and location is estimated by substituting the estimated transmittance for τ in Eq. (3). Then, the weighting function at the global scale is estimated as the spatial and temporal average of the estimated weights, and is shown in Fig. 4. For the other two models [MRI-CGCM3 and CanESM2 (Canadian Earth System Model version 2)] with 22 discrete pressure levels, the top of the model atmosphere is at 1 hPa. Their weight functions are estimated by using a similar approach as the other models, and are shown in Fig. 5.

It can be seen in Fig. 4 that the models' weighting functions are almost overlapped. So, a uniform weighting function for the models with 10 hPa as the TOA can be defined as the average of the weighting functions for these models. The weighing function for models with 1 hPa as the TOA can be constructed using a similar approach. This demonstrates that weighting functions with different discrete levels at 10 hPa or 1 hPa as the TOA give different vertical distributions. In this study, they are denoted by the proposed weighting functions.

Using Eq. (1), the weighting functions of RSS and UAH are assigned at the vertical levels of the models with the TOA at 10 hPa and at 1 hPa, respectively, and the corresponding profiles are shown in Figs. 4 and 5, respectively. Clearly, these two profiles are different from the proposed weighting functions.

4.2 *Linear trend analysis*

In this subsection, we compare the simulated T4 trends using static weighting function and RTTOV. For this purpose, four annual time series of the globally averaged T4 for each model are produced using UAH, RSS and the proposed weighting functions (shown in Figs. 4 and 5), and are calculated by RTTOV directly. Their linear trends are estimated using the approach documented in section 3.3.

The scatter plots between simulated T4 trends using the RSS weighting function and calculated by RTTOV are shown in Fig. 6. It shows that simulated T4 trends using the RSS weighting function are all larger than those calculated by RTTOV, with a systematic positive difference of 0.045 K $(10\ \mathrm{yr})^{-1}$ (Table 2). The scatter plots between simulated T4 trends using the UAH weighting function and calculated by RTTOV are shown in Fig. 7. Again, simulated T4 trends using the UAH weighting function are all larger than those calculated by RTTOV, but with a smaller systematic positive difference of 0.032 K $(10\ \mathrm{yr})^{-1}$ (Table 2).

Scatter plots between simulated T4 trends using the proposed weighting function and calculated by RTTOV are shown in Fig. 8. In this case, there is no systematic difference between trends estimated using the two approaches (Table 2).

Table 2. Multimodel mean trends for T4 using weighting functions and those calculated by RTTOV, and satellite-observed trends for T4 by groups at UAH, RSS and STAR [units: K (10 yr)$^{-1}$]. The analysis period is January 1979 to December 2005.

	UAH v5.4 (Obs.)	RSS v3.3 (Obs.)	STAR v2.0 (Obs.)	Using RSS WF	Using UAH WF	Using Proposed WF	Calculated by RTTOV v10
Globe	−0.439	−0.347	−0.370	−0.248	−0.262	−0.289	−0.294
Tropics	−0.403	−0.346	−0.419	−0.214	−0.242	−0.301	−0.285
Northern extratropics	−0.546	−0.376	−0.409	−0.245	−0.261	−0.285	−0.277
Southern extratropics	−0.416	−0.354	−0.340	−0.249	−0.262	−0.281	−0.308

5. Discussion and conclusions

5.1 *Simulated trend*

In this subsection, we focus on the T4 trends in 11 CMIP5 climate model simulations. We investigate the differences among the trends using the three static weighting functions (RSS, UAH and proposed) and that calculated by RTTOV, and especially, the causes of these differences.

From Table 2, the difference between the simulated T4 trends using the RSS (or UAH) weighting function and that calculated by RTTOV is 0.04 K (10 yr)$^{-1}$ [or 0.027 K (10 yr)$^{-1}$], which is about 10% larger than that of the averaged trend calculated by RTTOV.

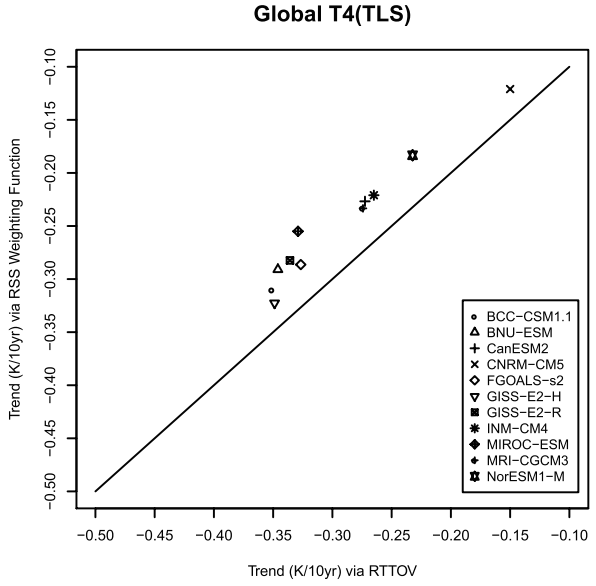

Fig. 6. Scatter diagram of MSU T4 trends from 11 climate models calculated by RTTOV v10 and generated using the RSS weighting function. Each trend of a climate model is averaged from the trends of the model's historical realizations. All trends are statistically significant (α=0.05). The analysis period is January 1979 to December 2005, the period of maximum overlap between the observations and CMIP5 model historical simulations.

Therefore, for better evaluating the simulated CMIP5 T4 trends, these differences may need to be corrected.

For investigating the causes of the differences, vertical global trends of air temperature for multimodel historical simulations from 1979–2005 are shown in Fig. 8. It can be seen that the trends are unevenly distributed at the vertical levels. From the surface to 150 hPa, the troposphere layer warms with an averaged trend of 0.22 K (10 yr)$^{-1}$ in the layer; from 150–60 hPa, the stratosphere increases the cooling trend; from 60–10 hPa, air temperature trends are almost stable [−0.5 K (10 yr)$^{-1}$]; and from 10 hPa, temperature trends increase linearly and reach about −1.4 K (10 yr)$^{-1}$ at the top of the model atmosphere (1 hPa).

For the static weighting function method, T4 is estimated as the weighted average of the CMIP5 model simulated temperature at all model levels contribution of the temperature trend at that level is made to the T4 trend. Figures 4 and 5 show that above (or below) 70 hPa, the RSS weights are systematically smaller

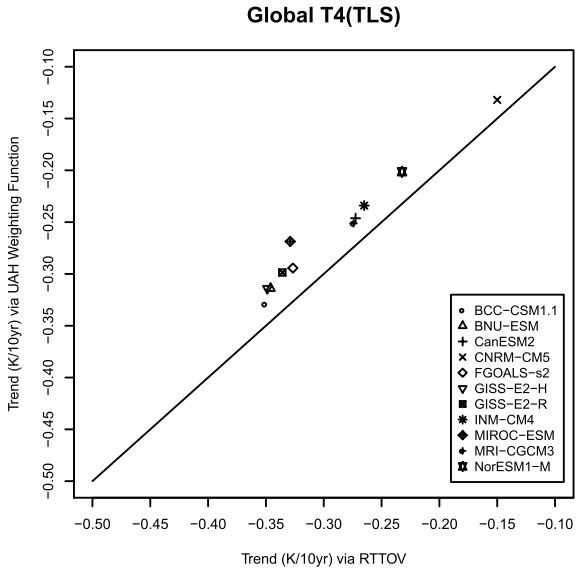

Fig. 7. The same as Fig. 6, but for simulated T4 trends using the UAH weighting function or calculated by RTTOV v10.

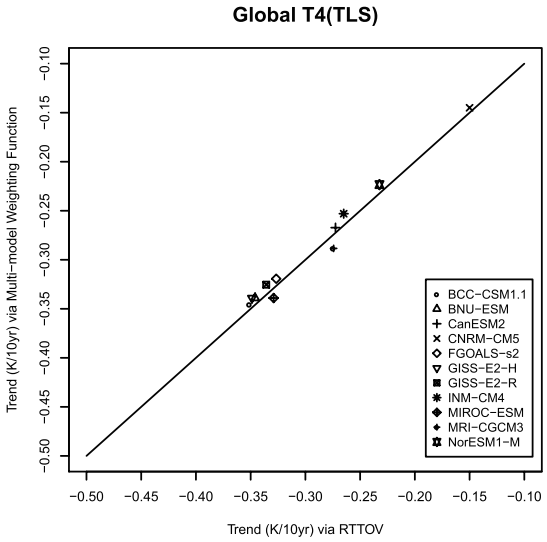

Fig. 8. The same as Fig. 6, but for simulated T4 trends using the multimodel proposed weighting function or calculated by RTTOV v10.

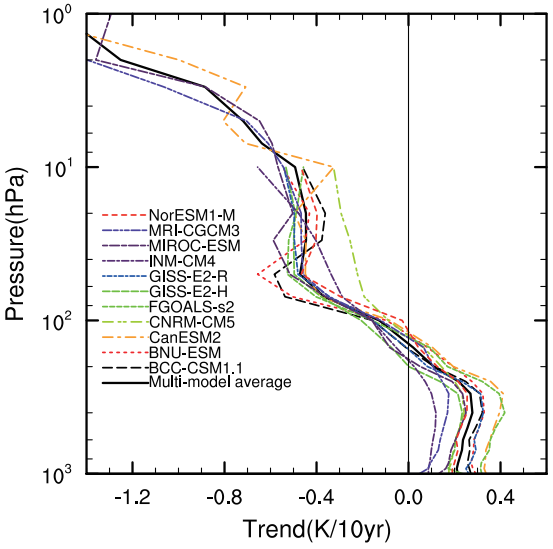

Fig. 9. Vertical distribution of trends of air temperature for multimodel historical simulations on global scales from 1979–2005. Only the first realization is plotted from each model.

(or larger) than model weights. From Fig. 9, the temperature trends above 70 hPa are more cooling than those below 70 hPa. Therefore, the CMIP5 T4 trends using RTTOV should be more cooling than those using the static RSS weighting function. This is also true for the UAH weighting function, but with smaller magnitude.

The RSS and UAH static weights have also been applied for estimating T4 trends in the tropics. For investigating the impacts of the three static weighting functions on regional T4 trends, the T4 trends over the tropics, the northern extratropics and southern extratropics are estimated using the three weighting functions respectively, as well as calculated by RTTOV, and are shown in Table 2. Over the tropics, the T4 trend estimated using the RSS (or UAH) weighting function constitutes about 0.09 K/decade [or 0.06 K $(10\ \mathrm{yr})^{-1}$] less cooling than the T4 trend estimated by RTTOV. This may be due to the weighting functions shown in Fig. 3 that are constructed based on U.S. standard atmosphere, and the tropopause over the tropics is higher than that over the northern extratropics. Since temperature trends in the troposphere are generally positive, the T4 trends estimated using the RSS and UAH weighting functions yield less cooling over the tropics than that estimated by RTTOV. Table 2 also shows that the differences in simulated T4 trends over the northern extratropics are less compared to the trends calculated by RTTOV. This may be due to the simulated CMIP5 models' tropopauses over the northern extratropics being closer to the tropopause of the U.S. standard atmosphere.

5.2 *Observed and simulated trends*

Table 2 shows that the averaged T4 trend simulated using the 11 CMIP5 climate models (generated by using either the RTTOV or the proposed weights) is about -0.30 K $(10\ \mathrm{yr})^{-1}$, while the calculated trend of the satellite-observed T4 derived by the UAH group is about -0.439 ± 0.114 K $(10\ \mathrm{yr})^{-1}$. The latter constitutes a significantly greater cooling trend than the former. Trends of the satellite-observed T4 derived by the STAR group and RSS group are -0.37 ± 0.11 K $(10\ \mathrm{yr})^{-1}$ and -0.347 ± 0.108 K $(10\ \mathrm{yr})^{-1}$, respectively. They are still different from the averaged T4 trend simulated using the 11 CMIP5 models, but to a lesser extent. Compared with the averaged T4 trends simulated by the 11 CMIP5 models using the UAH weighting function [-0.27 K $(10\ \mathrm{yr})^{-1}$] and the RSS weighting function [-0.26 K $(10\ \mathrm{yr})^{-1}$], the differences are even larger.

To further investigate whether or not the T4 trends of multimodel simulations are less cooling than the satellite-observed trends, the radiosonde observation datasets HadAt2 (Thorne et al., 2005a) for 1979–2002 are used as an independent test. Based on Thorne et al. (2005a), the global atmosphere was estimated to have warmed by about 0.1 K $(10\ \mathrm{yr})^{-1}$ from 850–250 hPa and cooled by about -0.5 K $(10\ \mathrm{yr})^{-1}$ from 300–30 hPa, and the maximum cooling trend was -1.0 K $(10\ \mathrm{yr})^{-1}$ at 30 hPa. Compared with the temperature trends simulated by the 11 CMIP5 models, the trends in the radiosonde observations is less warming in the troposphere, and more cooling in the stratosphere.

Therefore, the simulated T4 trend seems less cooling than those in the radiosonde observations. Since the T4 trends simulated by the 11 CMIP5 models are less cooling than the trends in satellite and radiosonde observations, they could be underestimated.

5.3 *Conclusions*

The latest version of the radiative transfer code (RTTOV v10) has been used to calculate the brightness temperature in the lower stratosphere (T4). It was found that the CMIP5 model-simulated T4 trends using the traditional UAH or RSS static weighting functions are less cooling than those calculated by RTTOV v10. Since the static weighting function approach is computationally more efficient and easier to apply than the approach using radiative transfer codes, a new static weighting function has been obtained from CMIP5 multimodel simulations and RTTOV. This proposed weighting function gives more weight to the stratosphere and less weight to the troposphere than the UAH (or RSS) weighting function. It has been demonstrated that the simulated T4 trends over the globe and over the tropics using the proposed weighting function are equivalent to those calculated by RTTOV.

The CMIP5 model-simulated T4 trends using the UAH and RSS weighting functions are less cooling than the trends of satellite-observed T4 constructed by the UAH group, RSS group and STAR group of radiosonde observations. The differences between the trends are reduced using our proposed static weighting function, but the problem remains, especially over tropics. In the future, we plan to continue investigating the reasons for the trend differences to see whether they are physically based (e.g. due to radiative forcing or modeling error, such as the inaccurate weighting functions discussed in this study), or due to other technical reasons (such as MSU data calibration). This is important in order to develop our understanding of climate change in the lower stratosphere.

Acknowledgements. This work was supported by the National Program on Key Basic Research Projects of China (Grant Nos. 2010CB951604 and 2010CB28402). We would like to thank Dr. Zhian SUN and the two anonymous reviewers for their valuable comments which lead to much improvement of this paper.

APPENDIX A

Proof for Eq. (3)

As described by Eq. (7.5.6) in Liou (2002), the brightness temperature $T_{\rm B}(\upsilon)$ at microwave frequency υ can be defined as

$$T_{\rm B}(\upsilon) = \varepsilon_\upsilon T_{\rm S}\tau_\upsilon(p_{\rm S},0) + (1-\varepsilon_\upsilon)\tau_\upsilon(p_{\rm S},0)\int_0^{p_{\rm S}} T(p)\frac{\partial\tau_\upsilon(p_{\rm S},p)}{\partial p}dp + \int_{p_{\rm S}}^{0} T(p)\frac{\partial\tau_\upsilon(p,0)}{\partial p}dp\,, \quad \text{(A1)}$$

where $T_{\rm B}(\upsilon)$ is the brightness temperature, ε_υ represents the surface emissivity, $T_{\rm S}$ is the skin temperature, $\tau_\upsilon(p_{\rm S},0)$ is the transmittance from surface to the TOA, and $T(p)$ is a temperature profile. The first terms on the right-hand sides of Eq. (A1) describe the contribution of surface emission. The second terms are the reflected emission from the surface to the TOA, and the third terms account for the contribution of atmospheric emission. For MSU channel 4, the absorption frequency in the lower stratosphere, the transmittance from surface to the TOA $\tau_\upsilon(p_{\rm S},0)$ is 0. Then, the contribution of the first item and second item in Eq. (A1) can be neglected. Therefore, we have

$$\begin{aligned} T_{\rm B}(\upsilon) &= \int_{p_{\rm S}}^{0} T(p)\frac{\partial\tau_\upsilon(p,0)}{\partial p}dp \\ &= \int_{\tau_{\rm s}}^{1} T(p)d\tau_\upsilon(p,0) \\ &\approx \sum_{l_p=1}^{nl_p} T(l_p)\frac{1}{2}\left[\tau(l_p+1)-\tau(l_p-1)\right] \end{aligned}\,, \quad \text{(A2)}$$

where $\tau(l_p)$ represents the transmittance from the specific pressure level to the TOA at the frequency υ. So, the weight for the l_pth level for MSU channel 4 is

$$W(l_p) = \frac{1}{2}\left[\tau(l_p+1)-\tau(l_p-1)\right]\,. \quad \text{(A3)}$$

REFERENCES

Becker, R. A., John M. Chambers, and A. R. Wilks, 1988: *The New S Language*, Chapman & Hall, New York. 132pp.

Christy, J. R., R. W. Spencer, W. B. Norris, and W. D. Braswell, 2003: Error estimates of version 5.0 of MSU-AMSU bulk atmospheric temperatures. *J. Atmos. Oceanic Technol.*, **20**, 613–629.

Christy, J. R., W. B. Norris, R. W. Spencer, and J. J. Hnilo, 2007: Tropospheric temperature change since 1979 from tropical radiosonde and satellite measurements. *J. Geophys. Res.*, **112**, D06102, doi: 10.1029/2005JD006881.

Douglass, D. H., B. D. Pearson, and S. F. Singer, 2004: Altitude dependence of atmospheric temperature trends: Climate models versus observations. *Geophys. Res. Lett.*, **31**, L13208, doi: 10.1029/2004/GL020103.

Douglass, D. H., J. R. Christy, B. D. Pearson, and S. F. Singer, 2007: A comparison of tropical temperature trends with model predictions. *Int. J. Climatol.,* **27**, doi: 10.1002/joc.1651.

Grody, N. C., 1983: Severe storm observations with the microwave sounding unit. *J. Climate Appl. Meteor.*, **22**, 609–625.

Grody N. C., K. Y. Vinnikov, M. D. Goldberg, J. T. Sullivan, and J. D. Tarpley, 2004: Calibration of multisatellite observations for climatic studies: Microwave sounding unit (MSU). *J. Geophys. Res.*, **109**, D24104, doi: 10.1029/2004JD005079.

IPCC, 2007: Summary for policymakers. *Climate Change 2007: The Physical Science Basis, Contribution of Working Group I to the Fourth Assessment Report of the Intergovernmental Panel on Climate Change*, S. Solomon et al., Eds., Cambridge University Press, Cambridge, New York, 2–14.

Jones, P. D., 1989: The influence of ENSO on global temperatures. *Climate Monitor*, **17**, 80–90.

Liou, K. N., 2002: Application of radiative transfer principles to remote sensing. *An Introduction to Atmosphere Radiation*, 2nd ed. K. N. Liou, Ed., Academic Press, San Diego, 414–418.

Matricardi, M., 2005: The inclusion of aerosols and clouds in RTIASI, the ECMWF fast radiative transfer model for the infrared atmospheric sounding interferometer. ECMWF Tech. Memo. 474, 53pp. [Available online at http://www.ecmwf.int/publications.]

Matricardi, M., 2008: The generation of RTTOV regression coefficients for IASI and AIRS using a new profile training set and a new line-by-line database. ECMWF Tech. Memo. 564, 47pp. [Available online at http://www.ecmwf.int/publications.]

Matricardi, M., F. Chevallier and S. Tjemkes, 2001: An improved general fast radiative transfer model for the assimilation of radiance observations. ECMWF Research Dept. Tech. Memo., 345pp. [Available online at http://www.ecmwf.int/publications.]

Mears, C. A., and F. J. Wentz, 2005: The effect of drifting measurement time on satellite-derived lower tropospheric temperature. *Science*, **309**, 1548–1550, doi: 10.1126/science.1114772.

Mears, C. A., and F. J. Wentz, 2009: Construction of the remote sensing systems V3.2 atmospheric temperature records from the MSU and AMSU microwave sounders. *J. Atmos. Oceanic Technol.*, **26**, 1040–1056, doi: 10.1175/2008JTECHA1176.1.

Mears, C. A., M. C. Schabel, and F. J. Wentz, 2003: A reanalysis of the MSU channel 2 tropospheric temperature record. *J. Climate*, **16**, 3650–3664.

Santer B. D., 1996: A search for human influences on the thermal structure of the atmosphere. *Nature*, **382**, 39–46.

Santer, B. D., J. J. Hnilo, T. M. L. Wigley, J. S. Boyle, C. Doutriaux, M. Fiorino, D. E. Parker, and K. E. Taylor, 1999: Uncertainties in observationally based estimates of temperature change in the free atmosphere. *J. Geophys. Res.*, **104**, 6305–6333.

Santer, B. D., T. M. L. Wigley, J. S. Boyle, D. J. Gaffen, J. J. Hnilo, D. Nychka, D. E. Parker, and K. E. Taylor, 2000: Statistical significance of trends and trend differences in layer-average atmospheric temperature time series. *J. Geophys. Res.*, **105**, 7337–7356.

Santer, B. D., and Coauthors, 2005: Amplification of surface temperature trends and variability in the tropical atmosphere. *Science*, **309**, 1551–1556.

Santer, B. D., and Coauthors, 2008: Consistency of modelled and observed temperature trends in the tropical troposphere. *Inter. J. Climatol.,* **28**, 1703–1722, doi: 10.1002/joc.1756.

Saunders, R., M. Matricardi, and P. Brunel, 1999: An improved fast radiative transfer model for assimilation of satellite radiance observations. *Quart. J. Roy. Meteor. Soc.,* **125**(556), 1407–1425.

Seidel, D. J., and Coauthors, 2004: Uncertainty in signals of large-scale climate variations in radiosonde and satellite upper-air temperature datasets. *J. Climate*, **17**, 2225–2240.

Spencer, R. W., and J. R. Christy, 1990: Precise monitoring of global temperature trends from satellites. *Science*, **247**, 1558–1562.

Spencer, R. W., and J. R. Christy, 1992a: Precision and radiosonde validation of satellite gridpoint temperature anomalies. Part I: MSU channel 2. *J. Climate*, **5**, 847–857.

Spencer, R. W., and J. R. Christy, 1992b: Precision and radiosonde validation of satellite gridpoint temperature anomalies. Part II: A tropospheric retrieval and trends during 1979–1990. *J. Climate*, **5**, 858–866.

Spencer, R. W., and J. R. Christy, 1993: Precision lower stratospheric temperature monitoring with the MSU: technique, validation and results 1979–1991. *J. Climate.*, **6**, 1194–1204.

Steiner, A. K., G. Kirchengast, M. Borsche, U. Foelsche, and T. Schoengassner, 2007: A multi-year comparison of lower stratospheric temperatures from CHAMP radio occultation data with MSU/AMSU records. *J. Geophys. Res.*, **112**, D22110, doi: 10.1029/2006JD008283.

Taylor, K. E., R. J. Stouffer, and G. A. Meehl, 2009: A summary of the CMIP5 experiment design. PCDMI Rep., 33pp., [Available online at http://cmip-pcmdi.llnl.gov/cmip5/docs/Taylor_CMIP5_design.pdf.]

Taylor, K. E., R. J. Stouffer, and G. A. Meehl, 2012: An overview of CMIP5 and the experiment design. *Bull. Amer. Meteor. Soc.*, 485–498, doi: 10.1175/BAMS-D-11- 00094.1.

Thorne, P. W., D. E. Parker, S. F. B. Tett, P. D. Jones, M. McCarthy, H. Coleman, and P. Brohan. 2005a: Revisiting radiosonde upper air temperatures from 1958 to 2002. *J. Geophys. Res.*, **110**, D18105, doi: 10.1029/2004JD005753.

Thorne, P. W., D. E. Parker, J. R. Christy, and C. A. Mears, 2005b: Uncertainties in climate trends: Lessons from upper-air temperature records. *Bull. Amer. Meteor. Soc.*, **86**, 1437–1442.

Vinnikov, K. Y., and Grody, N. C. 2003: Global warming trend of mean tropospheric temperature observed by satellites. *Science*, **302**, 269–272.

Vinnikov, K. Y., N. C. Grody, A. Robock, R. J. Stouffer, P. D. Jones, and M. D. Goldberg, 2006: Temperature trends at the surface and in the troposphere. *J. Geophys. Res.*, **111**, D03106, doi: 10.1029/2005JD006392.

Wigley, T. M. L., V. Ramaswamy, J. R. Christy, J. R. Lanzante, C. A. Mears, B. D. Santer, and C. K. Folland, 2006: *Executive summary in temperature trends in the lower atmosphere: Steps for understanding and reconciling differences*. T. R. Karl, S. J. Hassol, C. D. Miller, and W. L. Murray, Eds., A Report by the Climate Change Science Program and the Subcommittee on Global Change Research, Washington, DC, 2–13.

Zheng, X., and R. E. Basher, 1999: Structural time series models and trend detection in global and regional temperature series. *J. Climate*, **12**, 2347–2358.

Zou, C. Z., M. D. Goldberg, Z. Cheng, N. C. Grody, J. T. Sullivan, C. Cao, and D. Tarpley, 2006: Recalibration of microwave sounding unit for climate studies using simultaneous nadir overpasses. *J. Geophys. Res.*, **111**, D19114, doi: 10.1029/2005JD006798.

Zou, C. Z., M. Gao, and M. Goldberg, 2009: Error structure and atmospheric temperature trend in observations from the microwave sounding unit. *J. Climate*, **22**, 1661–1681.